SiF 2020– The 11th International Conference on Structures in Fire

The University of Queensland, Brisbane, Australia, November 30-December 2, 2020 (Author's Copy)

EXPERIMENTAL STUDY ON FIRE RESISTANCE OF A FULL-SCALE COMPOSITE FLOOR ASSEMBLY IN A TWO-STORY STEEL FRAMED BUILDING

Lisa Choe[1,*], Selvarajah Ramesh[2], Xu Dai[3], Matthew Hoehler[4], Matthew Bundy[5]

ABSTRACT

This paper presents the first of four planned fire experiments of a full-scale two-story steel framed building constructed at the National Fire Research Laboratory. This first experiment was aimed to quantify the fire resistance and behaviour of the steel composite floor system commonly built in the United States, incorporating prescriptive approaches for a 2-hour fire resistance rating. The 9.1 m × 6.1 m composite floor assembly, situated in the edge bay on the first floor of the prototype building, was tested to failure under a natural gas fuelled compartment fire and simultaneously applied mechanical loads. The test showed that the protected floor beams and girders of the test assembly achieved matching or superior fire resistance based on the acceptance criteria of standard furnace testing. However, the test floor slab exhibited a potential fire hazard within a specified fire rating period because of the use of a minimum code-compliant shrinkage reinforcement (59 mm^2/m). The heated slab cracked around the interior edges of the test bay less than 30 min into heating, followed by centre cracks along the secondary beam at 70 min. This centre breach, accompanied by ruptures of wire reinforcement, was caused by tension (due to catenary action) developed along the shorter span of the test floor assembly. This result suggests that the minimum slab reinforcement prescribed for normal conditions may not be sufficient to activate tensile membrane action of a composite floor system under the 2-hour standard fire exposure.

Keywords: Composite floors; steel buildings; fire resistance; compartment fire experiments

1 INTRODUCTION

There is lack of experimental data quantifying the fire performance of full-scale composite steel frames designed in accordance with United States (U.S.) building codes and specifications. Standard fire testing of the full-scale composite floor assemblies, incorporating both steel member connections and slab continuity, are extremely rare due to the size limitations of testing furnaces. The National Institute of Standards and Technology (NIST) is conducting a multi-year experimental test program to quantify the behaviour and limit states of full-scale structural steel frames with composite floors under compartment fire conditions. This test program consists of two parts: Phase 1 covers 12.8 m long composite beams with

[1] Research Structural Engineer, National Institute of Standards and Technology (NIST)
e-mail: lisa.choe@nist.gov, ORCID: https://orcid.org/0000-0003-1951-2746 (corresponding author)
[2] Foreign Guest Researcher, National Institute of Standards and Technology (NIST)
e-mail: selvarajah.ramesh@nist.gov, ORCID: https://orcid.org/0000-0002-9525-6767
[3] Foreign Guest Researcher, National Institute of Standards and Technology (NIST)
e-mail: xu.dai@nist.gov, ORCID: https://orcid.org/0000-0002-9617-7681
[4] Research Structural Engineer, National Institute of Standards and Technology (NIST)
e-mail: matthew.hoehler@nist.gov, ORCID: https://orcid.org/0000-0002-6049-7560
[5] Supervisory Mechanical Engineer, National Institute of Standards and Technology (NIST)
e-mail: matthew.bundy@nist.gov, ORCID: https://orcid.org/0000-0002-1138-0307

simple shear connections [1] and Phase 2 covers 9.1 m by 6.1 m composite floor assemblies in a two-story structural steel gravity frame. This paper presents the first experiment of the Phase 2 study conducted at NIST's National Fire Research Laboratory (NFRL) [2] on November 14, 2019. The test floor assembly was located on the first floor south-edge bay of the two-story prototype building and tested to failure under combined mechanical loads and a standard fire exposure simulated using natural gas burners. The objective of this test was to measure the structural and thermal responses of the composite floor assembly designed and constructed following the current U.S. prescriptive approach and to evaluate its system-level fire resistance based on the American Society of Testing and Materials (ASTM) standard E119 criteria [3]. The experimental results presented herein will serve as baseline to compare with the remaining experiments in Phase 2 and be used to guide the validation of computational models and design tools.

2 TEST STRUCTURE

The two-story structural steel frame was constructed to conduct a series of single-bay compartment fire experiments; see Figure 1(a). This test frame consisted of three bays by two bays in plan with a total floor area of 18 m × 11 m. The total height was approximately 7.2 m. The composite floor assembly was constructed on the first floor (3.8 m above the ground floor), whereas on the second floor a beam framing was erected without concrete slab. The same sizes of wide-flange steel shapes were used for both the first and second floor frames. Figure 1(b) shows the plan view of the protype building. All steel columns were W12×106 shapes typically used for reaction frames in the NFRL and anchored to the laboratory strong floor. The perimeter columns were continuous over two stories, whereas the two interior columns were spliced 92 cm above the concrete slab on the first floor. The 9.1 m long W16×31 beams in the fire test bay were connected to the column flange or at midspan of the 6.1 m long W18×35 girder using standard shear tabs; see Figure 2(a). Extended shear tabs were used at the ends of W18×35 girders; see Figure 2(b). All other beams and girders were connected using bolted angles and extended shear tabs, respectively. All structural steel shapes and shear tabs were rolled from A992 steel (a minimum specified yield strength of 345 MPa) and A36 steel (a mimimum specified yield strength of 250 MPa), respectively.

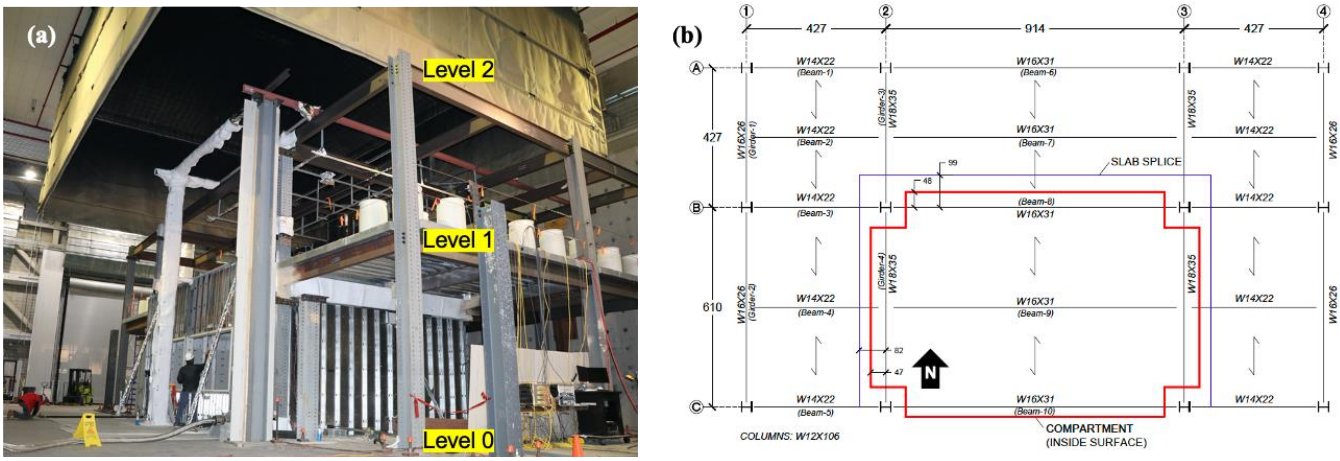

Figure 1. (a) Two-story prototype steel framed building; (b) Floor plan view (dimensions in cm).

The concrete slab was lightweight concrete (a minimum specified compressive strength of 28 MPa) cast on 76 mm deep formed steel decking. The concrete mixture included polypropylene fibres to minimize thermally induced spalling as suggested by Maluk at al. [4], which was also used for the Phase 1 composite beam study [5]. The concrete slab was cast approximately 5 months prior to fire testing. The moisture content of the concrete at time of fire testing was 7.6 % when measured according to ASTM C642-13 [6]. As shown in Figure 2(c), the slab thickness was 83 mm required for the 2-hour fire resistance rating with exposed steel deck. The cold-formed welded wire reinforcement of 59 mm^2/m, spaced at 152 mm, was embedded 41 mm below the top surface of the concrete slab. This is the minimum shrinkage reinforcement prescribed in the relevant U.S. design standard [7]. The floor slab was acting partially composite with steel beam assemblies through headed stud anchors (shaft Ø19 mm). For the W16×31 beams, a single headed

stud anchor was spaced at 305 mm; a pair of the same size stud anchors were welded atop the W18×35 girders at spacing of 356 mm, as shown in Figure 2(c). The corresponding degree of composite action was about 65 % of the ambient yield strength of the steel beams. In addition, the 77 cm long No. 4 hooked reinforcing bars (Ø13 mm) were placed perpendicular to the south edge beam under each stud to prevent separation of the heated concrete slab during the test. The slab splices along the interior edges of the test bay, shown in Figure 1(b), incorporated No. 4 bars and screw anchors so that the surrounding floor assemblies can be reused for subsequent fire tests. This splice design allows the full slab continuity (i.e., moment and shear transfer) between the test floor and the surrounding floor assemblies at ambient temperature. The construction detail at the northwest corner of the test bay is shown in Figure 3(a).

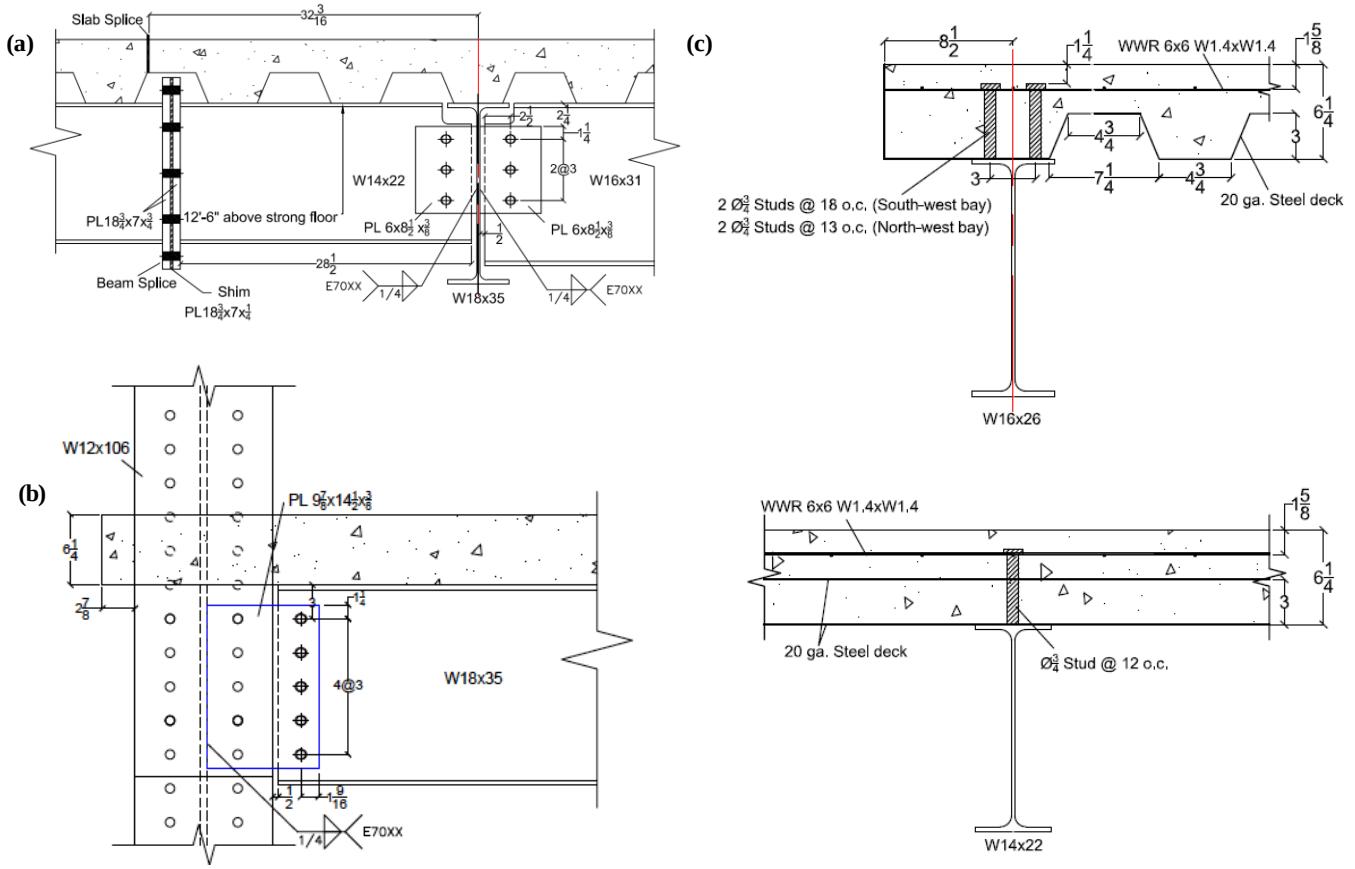

Figure 2. Details of (a) Standard shear-tab connection; (b) Extended shear-tab connection; (c) Composite sections. Dimensions in inch (1 in. = 2.54 cm)

Figure 3(b) shows a photograph of the fire test compartment, approximately 10 m long and 7 m wide. The height of the composite floor soffit was 377 cm above the compartment floor. The enclosing walls were constructed with 3 m tall sheet steel metals and a 48 mm thick gypsum board liner on the exposed wall surface. The 0.8 m gap between the compartment ceiling and the top edges of the three internal walls was lined with two layers of 25 mm thick ceramic blankets. Four natural gas burners (1.5 m × 1 m each) were distributed across the floor of the test compartment. The main vent was on the south wall, approximately 150 cm tall × 582 cm wide. There was a 30 cm tall × 582 cm wide slit on the north wall, designed for air intake only. The height of the windowsill on both the north and south walls was 100 cm above the strong floor.

The exposed steel frame within the test compartment, shown in Figure 1(b), was sprayed with a gypsum-based cementitious material (average specified density of 295 kg/m^3) for the 2-hour fire resistance rating. The average measured thickness of sprayed fireproofing prior to fire testing was 18 mm for both primary W16×31 beams and W18×35 girders and 13 mm for the secondary W16×31 beam. The coefficient of variation in thickness measurements was approximately 15 %. The exposed steel connections and columns were over sprayed with the same fireproofing material, with the thickness ranging from 25 mm to 28 mm.

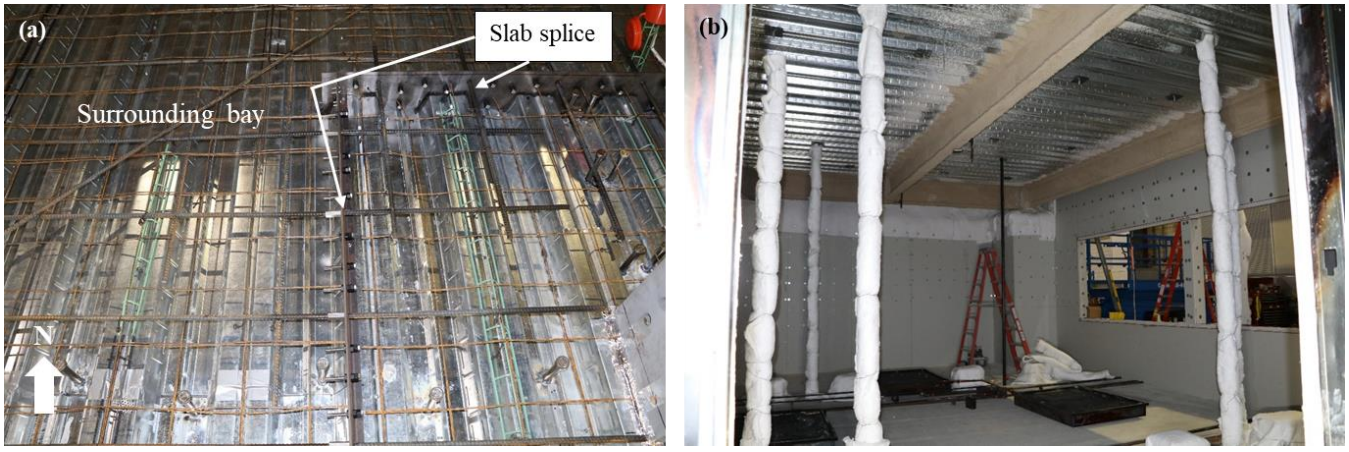

Figure 3. (a) Reinforcement details of slab splice; (b) Fire test compartment with the main vent on the south wall.

3 TEST CONDITIONS

The total mechanical load imposed on the 9.1 m × 6.1 m test floor assembly was approximately 150 kN (or 2.7 kPa), conforming to the American Society of Civil Engineers (ASCE) gravity load combination [8] of *1.2×dead load + 0.5×live load*. This load was distributed at twenty-four points across the test floor using water-cooled loading frames connected to four hydraulic actuators mounted in the basement, Figures 4(a) and 4(b). The total floor load including the assembly self-weight was approximately 5 kPa. The surrounding floors were loaded by water-filled drums, simulating a uniformly distributed mechanical load about 1.3 kPa. The load ratio (i.e., total load normalized by the ambient design capacity) of the test assembly was approximately 0.3 for both the secondary composite beam and the standard shear tabs of the same beam. The load ratio of the steel members and connections in the surrounding bays was less than 0.2.

The hydraulically loaded test floor assembly was exposed to a natural gas fuelled compartment fire, Figure 4(c), simulating the ASTM E119 time-temperature curve. Figure 4(d) shows the burner heat release rate (HRRburner) versus time relationship used in this test. This relationship was verified through a series of mock-up tests [10] conducted prior to this experiment. It should be noted that, as shown in Figure 4(d), there was a short loss (< 3 min) of the HRRburner data at 102 min due to network disruption of the natural gas delivery system. The fire and mechanical loads were removed at approximately 107 min. The total expanded uncertainty (with a coverage factor of 2 as defined in [11]) in measurements of the burner heat release rate and mechanical load is estimated 1.4 % at 10 MW [12] and 2 % at 150 kN, respectively.

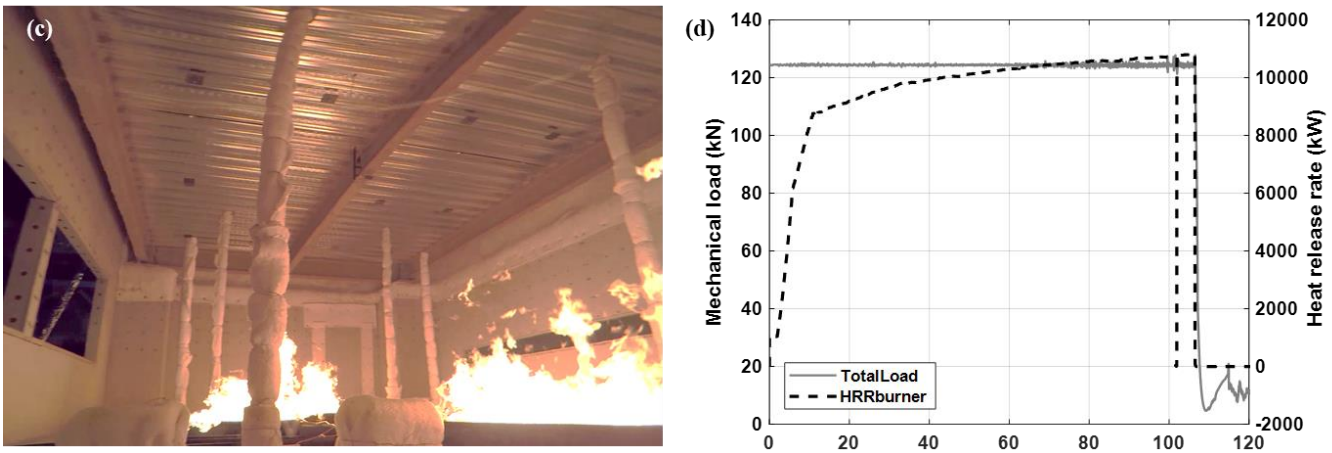

Figure 4. (a) Mechanical loading atop the test assembly; (b) hydraulic actuators mounted beneath the test compartment using yoke [9]; (c) compartment fire growth simulated with natural gas burners; (d) time history of total mechanical load (TotalLoad) and heat release rate of burners (HRRburner).

4 RESULTS AND OBSERVATIONS

4.1 Thermal response

Over two-hundred type K thermocouples (bead Ø 0.5 mm) were deployed at various locations across the test assembly. The average upper layer gas (ULG) temperature within the test compartment was measured using twelve Inconel-sheathed thermocouple probes hanging 305 mm below the steel deck. The average ULG temperature exceeded 700 °C at 11 min and reached a peak value of 1060 °C at 107 min. After 15 min from the burner ignition, the increase in the average ULG temperature resembled the International Organization for Standardization (ISO) standard 834 [13] temperature and was about 2 % higher than the ASTM E119 temperature. The standard deviation of temperatures measured using these thermocouples was less than 50 °C, indicating practically uniform temperatures below the test floor assembly.

Figure 5 illustrates the measured temperature rise in the midspan composite sections of the test assembly, Figure 2(c). For the W16×31 composite beams, the average temperature of the web and bottom flange of the protected steel beams reached 600 °C at 60 min and exceeded 800 °C at 107 min, Figure 5(a). The average concrete temperature at 0.5 mm above the top rib of the steel decking along the beam centrelines increased to 270 °C at 107 min. Temperatures of headed stud anchors at 38 mm above the top flange and welded wire reinforcement (WWR) remained below 400 °C and 200 °C, respectively.

For the W18×35 composite girders, as shown in Figure 5(b), the lower portion of the protected steel girders heated to 450 °C at 60 min and 700 °C at 107 min. The top flange steel temperature increased to 400 °C. The bottom concrete temperature in the shallow section next to the steel girder, Figure 2(c), increased to 600 °C at 80 min but significantly influenced by combined effects of concrete fractures and debonding of steel decking afterwards. The average temperatures of headed studs (at 2.5 cm above the steel decking) and WWR atop the girders never exceeded 300°C and 200 °C, respectively, during and after fire exposure.

The standard deviation in temperatures of the three heated W16×31 beams ranged from 60 °C to 110 °C, as indicated by error bars in Figure 5(a). This temperature variation might be caused by thermally induced fissures and degradation in coated insulation as the beams were undergoing severe thermal elongation and bending under fire loading. Unlike W16×31 beams, one can observe a smaller temperature difference (30 °C to 60 °C) between the east and west W18×35 girders, Figure 5(b). These girders seldom physically deformed, and thereby the applied fireproofing appeared to maintain relatively good integrity during fire loading.

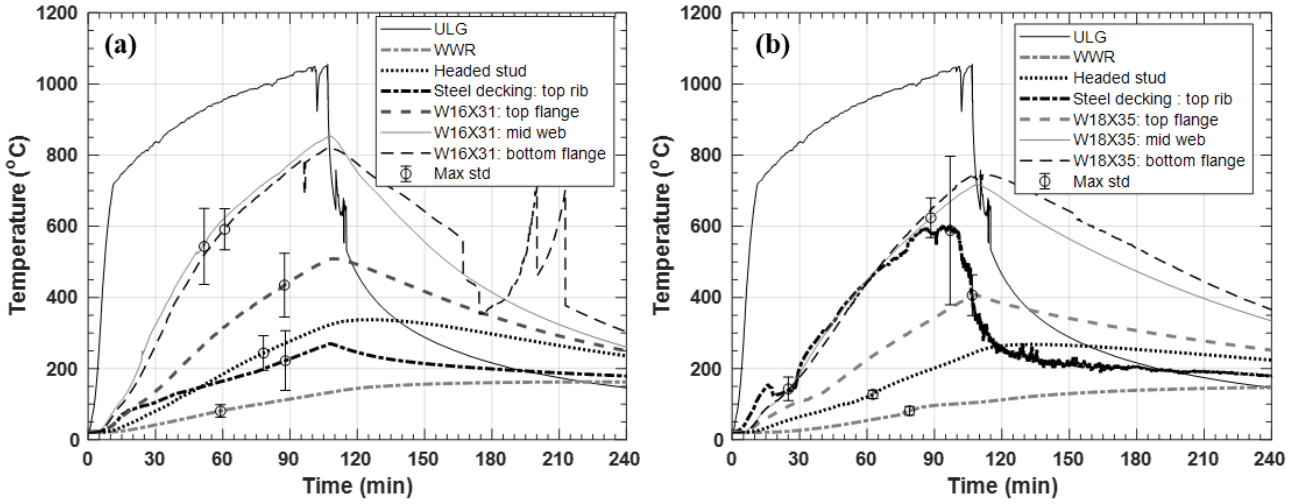

Figure 5. (a) Measured temperatures of (a) W16×31 composite beam and (b) W18×35 composite girder. Plotted with the average values of three W16×31 beams or two W18×35 girders in the test compartment.

A total of thirty-six thermocouples were mounted inside of the 9.1 m by 6.1 m test floor slab at various locations that were not thermally shaded by the steel framing underneath. Figure 6 shows the average concrete temperature in the deep (thickness = 159 mm) or shallow (thickness = 83 mm) sections of the concrete slab. Thermocouples installed at the steel decking (TST-5*) measured the hottest temperature, reaching nearly 900 °C during fire loading. The peak temperature of the concrete near the bottom rib of the steel decking (TST-4) was about 100 °C higher than the concrete temperature near the top rib (TST-7). However, the spatial temperature variation of TST-5* and TST-7 was quite high (> 110 °C), as indicated by the large error bars. These temperatures could be sensitive to debonding of the concrete from the steel decking. Temperatures of the WWR were affected by varying thickness of the concrete slab. At 107 min, for example, TST-1 (at deep sections) and TST-6 (at shallow sections) was 120 °C and 380 °C, respectively. In addition, the concrete temperatures towards the top surface (TST-1, TST-5, and TST-6) or at the centroid of the deep section (TST-2) were affected by moisture, as evidenced by the temperature plateau at 100 °C, over a longer period.

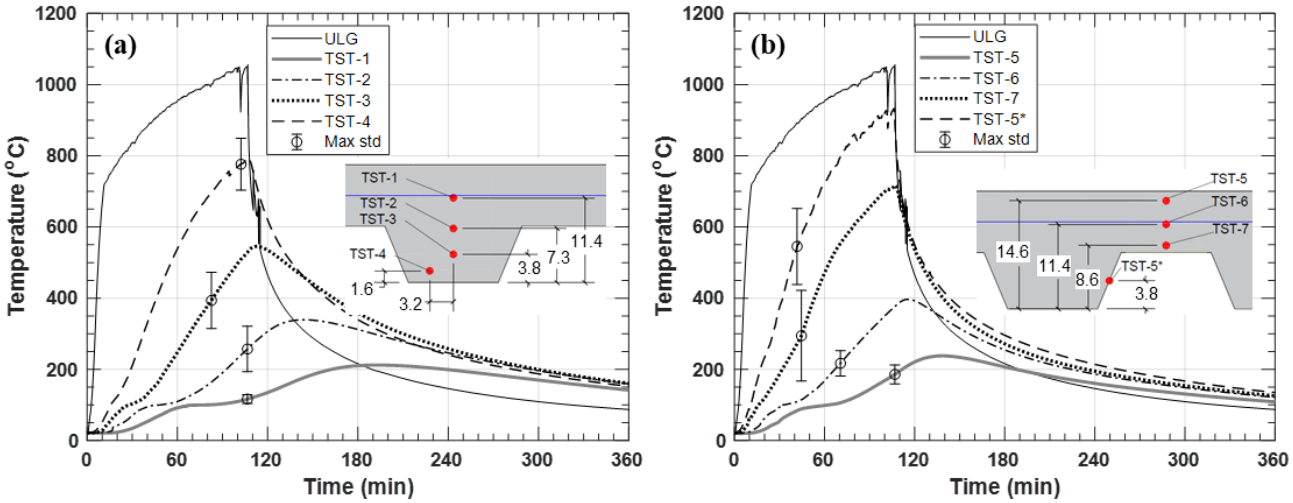

Figure 6. Measured temperatures of (a) deep section and (b) shallow section of the concrete floor slab. Plotted with the average values of six deep sections or four shallow sections across the test floor; thermocouple locations are in cm.

Although the data are not presented in this paper, the top (unexposed) surface temperature continued to rise during the cooling phase (up to 1 hour following extinguishment), ranging from 140 °C to 180 °C. Temperatures of the beam-to-girder shear-tab connection reached over 600 °C, whereas that of the shear-tab connections to columns were below 400 °C due to the thicker insulation sprayed on those regions. Detailed discussions and results of the connection temperatures are presented in the companion paper [14].

Estimates of total expanded uncertainty (with a coverage factor of 2) in measurements of the gas-phase, steel, and concrete temperatures are 8 % at 1110 °C, 4 % at 970 °C, and 6 % at 310 °C, respectively.

4.2 Structural response

The loaded test floor assembly continuously sagged during heating, while sequentially developing concrete fractures at various locations. No explosive spalling of the concrete was visible during or after the experiment, however, small 'popping' sounds continued during heating indicating that (micro) spalling was occurring between the bottom of the slab and the steel deck. Concrete surface cracks first appeared along the east and west girders as well as the north edge beam of the test bay about 20 min to 30 min after ignition. Around 40 min into heating, the southeast corner of the heated floor slab fractured making a loud noise. After 70 min, tensile fracture of the concrete was visible near the longitudinal (east-west) centreline of the test floor. Reaching 100 min in fire, small flames were intermittently visible above the top of the heated slab towards the east and west ends of this longitudinal crack, indicating failures of some screw joints of steel deck units in those locations. From this point forward, the mechanical loads on the south side of the test slab appeared to be supported by the steel deck and the south edge beam with concrete hanging cantilever, Figure 7(a). The fire and mechanical loading were removed at 107 min due to safety concerns.

A total of thirty displacement transducers were deployed to characterize the displacement of the two-story steel frame and the 9.1 m by 6.1 m test floor assembly during and after fire exposure. Figure 7(b) shows locations of the selected vertical and horizontal displacement sensors (labelled VD and HD, respectively) of the test assembly. All VD sensors in Figure 7(b) were located at the transverse (north-south) centreline of the test assembly. HD4 and HD6 sensors were used to measure thermal expansion at the perimeter of the heated floor assembly in the east-west direction and the north-south direction, respectively. HD9 measured the lateral displacement of the southeast column at the first story level. These horizontal displacement measurements were made at 15 cm above the top surface of the test floor slab. The total expanded uncertainty (with a coverage factor of 2) in measurements of the vertical and horizontal displacements is estimated 1 % at 580 mm and 5 % at 35 mm, respectively.

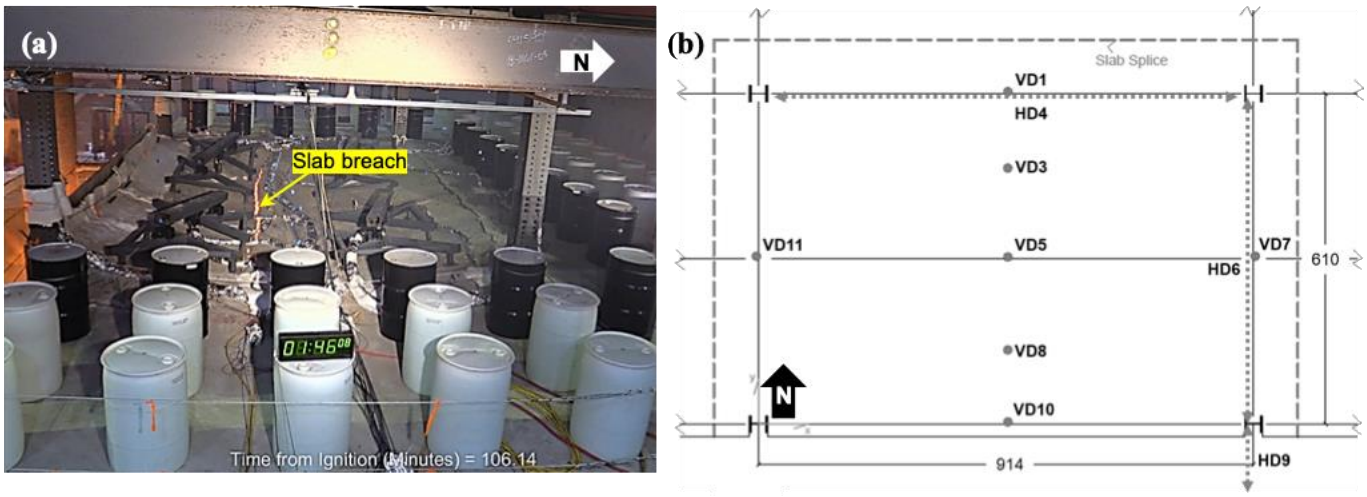

Figure 7. (a) Breach of the test floor slab; (b) Locations of displacement measurements with dimensions in cm.

As shown in Figure 8, the vertical displacement of the test floor assembly continuously increased during heating (until 107 min) and partly recovered during cooling; however, collapse did not occur. Until 60 min after ignition the values of VD5 and VD8 were similar. However, after the test floor slab began to breach (wide longitudinal crack) around 70 min, VD5 surpassed VD8 and reached 460 mm at 92 min. This displacement was approximately equal to the ratio of L/20 where L is the east-west span of 9.1 m. While VD5 finally reached the L/16 ratio at 107 min, there was no indication of 'runaway' deformation. Conversely, the vertical displacements of the perimeter steel members (VD1, VD7, VD10, and VD11) were relatively small, ranging from 65 mm to 210 mm. Also, VD7 and VD11 appeared to be less affected by the longitudinal concrete fractures. These perimeter members exhibited some degree of twisting and lateral deformations, discovered during the post-test inspections.

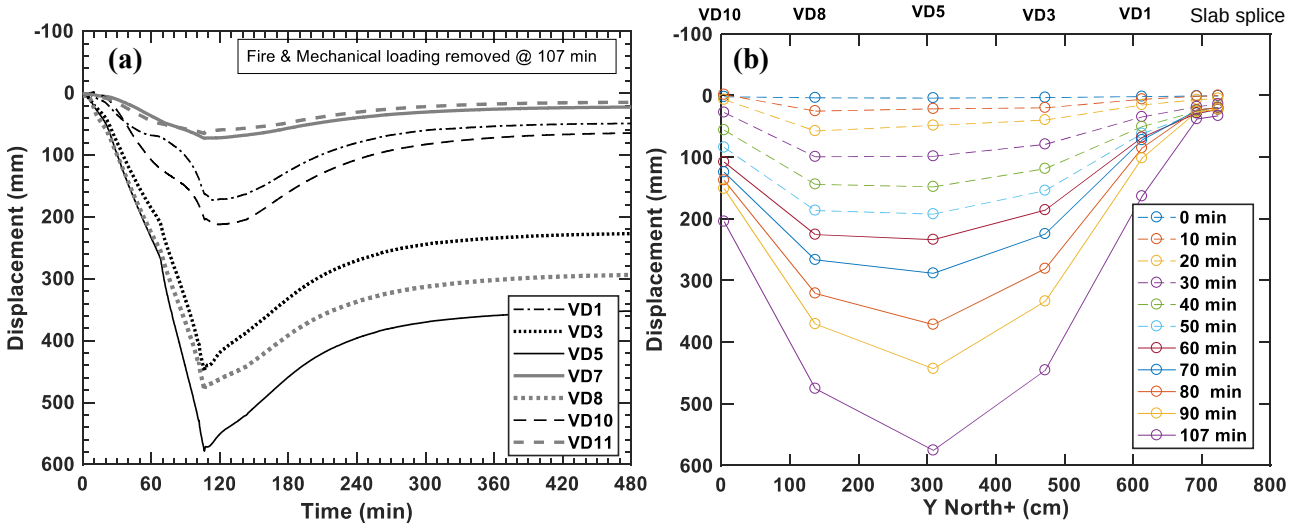

Figure 8. (a) Vertical displacements after the burner ignition at 0 min; (b) Vertical displacement profile varying with fire exposure time.

Figure 9(a) shows the midspan vertical displacements of fireproofing protected steel beams and girders as a function of the bottom flange temperatures. When the bottom flange temperature exceeded 700 °C, the vertical displacement of the secondary beam (VD5) increased much more rapidly from 0.4 mm/°C to 1.4 mm/°C. This change could be caused by several factors, such as initiation of a longitudinal breach of the test floor slab and continuous degradation of flexural strength and stiffness of support beams at higher temperatures. In the early stage of fire, on the other hand, the increase in displacements of the east and west girders (VD7 and VD11, respectively) was affected by smaller applied load ratios than the secondary beam. Furthermore, the heating rate of these members was relatively slow due to larger heat capacity and any heat loss associated with their close proximity to the upper wall lining with ceramic blankets or concrete fractures above these members. The vertical displacement of the south edge beam (VD10) was more responsive to the temperature change than other three perimeter members due to its free slab edge allowing less resistance to lateral-torsional buckling of this beam.

The horizontal (axial) displacements of the test assembly were measured using the lateral displacements of the columns at the first-story level. Figure 9(b) shows the time-varying horizontal displacement of the north primary beam (HD4) and the east girder (HD6) of the test assembly as well as the lateral displacement of the southeast column. The positive values in this figure represent the displacements due to thermal expansion of the heated test assembly. The values of HD6 and HD9 were similar throughout the test, indicating that the east girder expanded in single direction, towards the south due to a much larger restraint provided by the north surrounding frame. These displacements increased continuously to a peak value ranging from 32 mm to 34 mm until the fire test was terminated. The value of HD4 increased at a similar rate but began to decrease after 70 min when the longitudinal fracture of concrete occurred. The maximum axial displacement due to thermal expansion in the east-west direction was approximately 22 mm.

Figure 10 shows the final fracture pattern of the test floor slab after cooling. As mentioned earlier, concrete cracks developed along the north, east, and west edges of the test bay, followed by the longitudinal cracks 530 mm or less south of the secondary beam. Most of WWR (59 mm^2/m) across the thicker lines of fractures visible in Figure 10 completely ruptured. Neither concrete failures along the south (free) edge (i.e., separation from the south edge beam) nor slab splice failures were witnessed. Based on crack openings of the concrete, the east and west edge cracks were initiated near the flanges of the southeast and southwest columns, whereas the north edge crack was propagated from the midspan or its vicinity. No through-depth fractures were observed around the northeast and northwest columns.

The middle breach of the test floor slab appeared to be occurred due to catenary action in the north-south direction where the steel decking was continuous into the north adjacent bay. It is believed that the tensile membrane action of the test floor slab was not achieved or developed in a limited fashion because of the early formation of concrete fractures and ruptures of welded wire reinforcement along the east and west

edges. These through-depth cracks located 100 mm or less inside of the test-bay column grid, which formed shortly after fire ignition and continued to widen unchecked during heating. Thus, the headed stud anchors on the east and west girders were ineffective to induce tension in the concrete in the east-west direction as the heated floor slab continued to deflect downward. In contrast, the north edge crack formed 370 mm or less north of the north primary beam (i.e., outside of the test-bay column grid) and thereby the headed stud anchors on all three 9.1 m long beams appeared to provide anchorage of the concrete and steel decking against tension developing in the north-south direction. As the vertical displacement of the test floor increased in fire, the excessive tension would develop more effectively in the north-south direction than in the east-west direction until WWR finally ruptured at critical locations. This WWR rupture would happen in the concrete where the vertical displacements were greater, i.e., south of the secondary beam as shown in Figure 8(b).

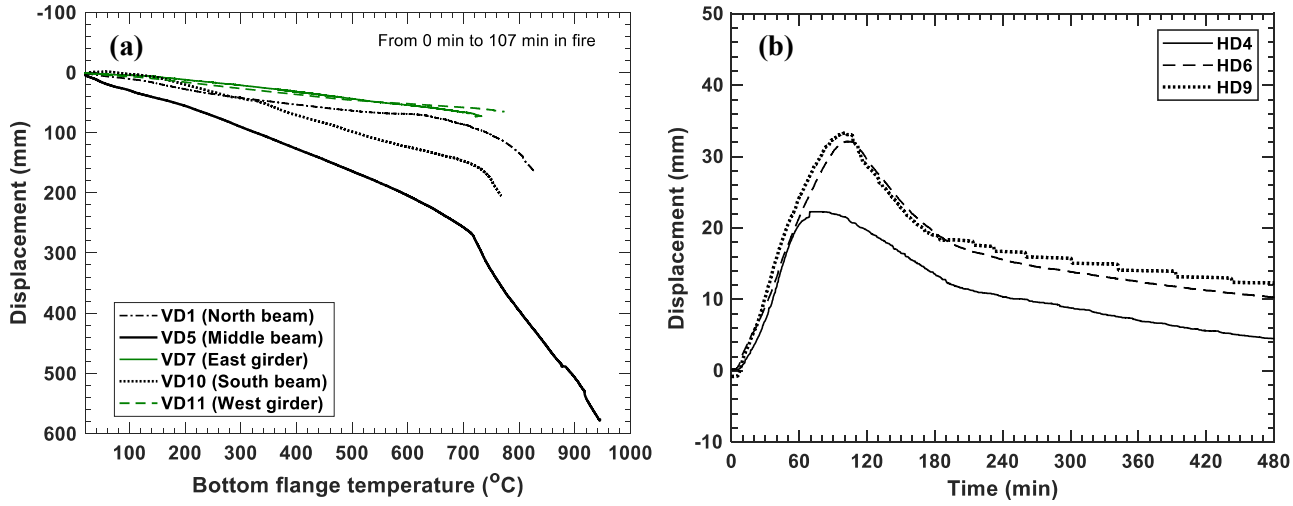

Figure 9. (a) Vertical displacement data as a function of bottom flange temperatures during heating; (b) Horizonal displacements measured at 15 cm above the test floor slab during heating (until 107 min) and cooling.

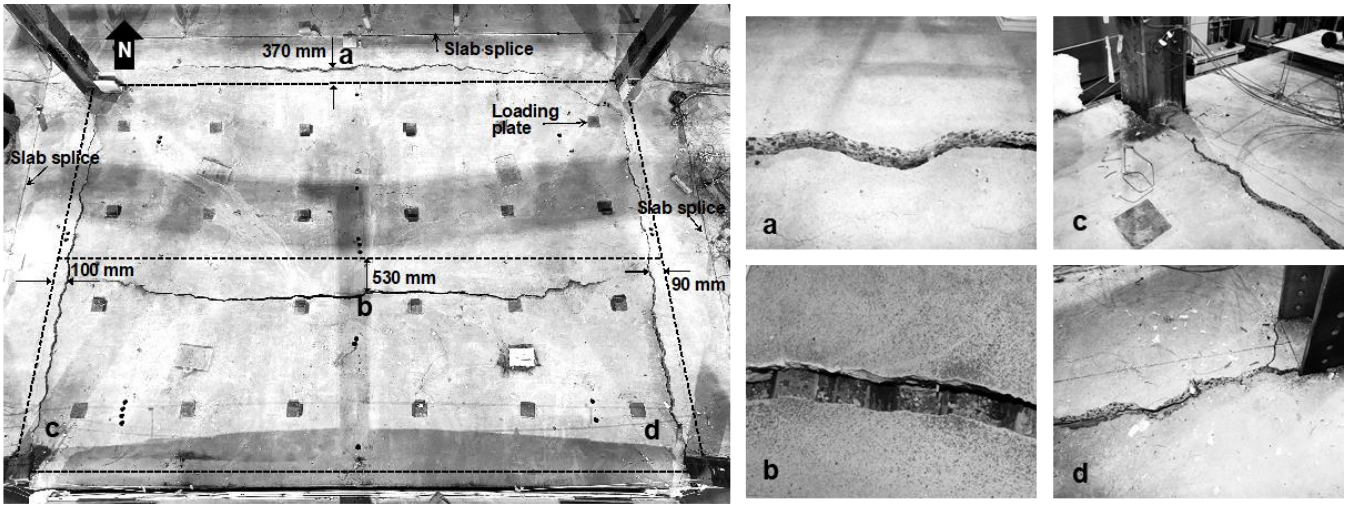

Figure 10. Top of the test floor slab after cooling. Dashed lines define the test-bay column grid. The four photographs on the right (a through d) show close-ups of concrete fractures.

Figure 11 shows the underside of the test floor assembly after cooling. The steel deck below concrete fractures (Figure 10) mostly maintained its integrity with good ductility. Only a local rupture was found in the deck unit below the east end of the mid-panel longitudinal crack, i.e., near the west edge of the top flange of the east girder. All three 9.1 m long W16×31 beams exhibited permanent strong axis bending deformation and local buckling near the beam ends. Furthermore, the north and south primary beams also exhibited twisting and lateral deformations. The end connections of these beams, however, maintained their structural integrity. The east and west W18×35 girders showed little residual vertical deflection and exhibited minor out-of-plane deformations in the webs near the end connections. The extended shear tabs

welded to the northeast and the northwest columns exhibited noticeable out-of-plane deflection but no bolt failures. The extended shear tabs welded to the southeast and the southwest columns deflected little, whereas there were partial shear ruptures in the lower bolts of the southeast connection. The sprayed fireproofing on the beams and girders mostly remained intact, although fissures were evident on the beam web near the end connections and at the lower beam web of the secondary beam at midspan.

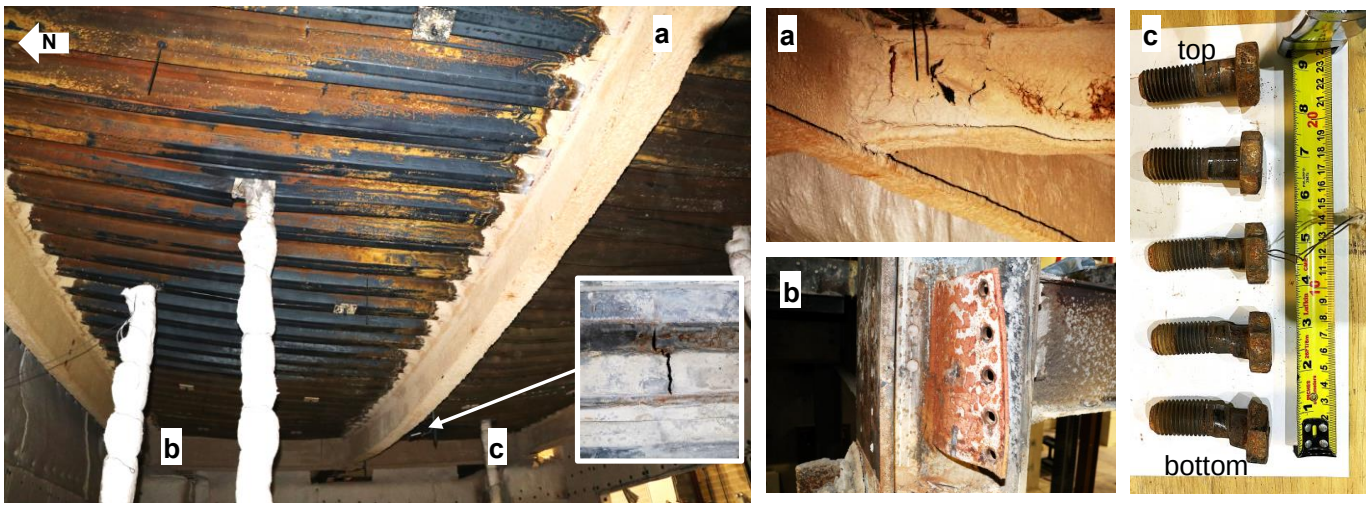

Figure 11. Fire-exposed steelwork of the test floor assembly after cooling. Close-ups of some deflected steel parts are shown in a through c.

4.3 Comparison with ASTM E119 criteria

The intent of standard fire testing, mostly performed using a purpose-built furnace, is to provide a consensus-based method to evaluate the duration for which an *isolated* floor assembly contains a fire while retaining its structural stability, the so-called *fire resistance rating* expressed in minutes or hours. This testing is typically performed using a test assembly with limited size (e.g., a minimum floor area of 16.7 m^2 and a minimum beam span of 3.7 m [3]) with two end support conditions, either *restrained* or *unrestrained* as explained in LaMalva et al [15]. A test assembly is required to resist its maximum load for normal conditions (e.g., *1.2×dead load + 1.6×live load* per ASTM E119 standard) while subjected to standard furnace heating. The fire resistance rating of a test assembly is usually determined based on limiting temperatures and displacements as discussed below.

Figure 12 summarizes the test results in comparison with ASTM E119 acceptance criteria. For the 2-hour *restrained* fire resistance rating, the test specimen must meet the following conditions: (i) sustaining the applied loads with no ignition of cotton waste placed on the top of the heated concrete slab during the full rating period, (ii) the average temperature on unexposed surface less than 139 °C above its initial temperature during the first hour, (iii) a peak temperature of structural steel members below 704 °C during the first hour, and (iv) the average temperature at any section of structural steel members below 593 °C during the first hour, and (v) the maximum total displacement less than the value of $Lc^2/400d$ where Lc = beam clear span, d = depth of composite beam, and the corresponding displacement rate less than the value of $Lc^2/9000d$. As shown in Figure 12, the protected individual W16×31 beams and W18×35 girders of the test assembly successfully met the limiting temperature and displacement criteria. The average concrete surface temperature measured by eight thermocouples distributed across the test assembly was approximately 120 °C prior to extinguishment of the fire. Although the maximum total displacement of the secondary beam exceeded the ASTM E119 displacement limit, the measured displacement rate of this beam was 40 % less than its specified value. It is important to note that this condition was achieved at the total floor load from the load combination of *1.2×dead load + 0.5×live load*, approximately 60 % of the maximum load condition (e.g., *1.2×dead load + 1.6×live load*) as prescribed in ASTM E119 [3].

Furthermore, this test has revealed some potential issues related to the integrity of a composite floor assembly as part of compartmentation under fire loading. As shown in Figure 13, the centre breach in the test floor slab, initiated prior to the specified rating period of 120 min, was accompanied by ruptures of the wire reinforcement in tension at the mid-panel displacement of 350 mm (L/26) or greater. A minimum

code-required amount of shrinkage reinforcement (59 mm^2/m) used in the test assembly was insufficient to resist thermally induced tension during the investigated fire. Although the steel deck continuously running in the transverse (north-south) direction of the test assembly appeared to be ductile at large vertical displacements, failure of side deck joints (screws failure at the decking overlap), local deck ruptures, exposure of the heated decking units within concrete cracks allowed the penetration of flames and hot gases beyond the test compartment. This condition could have potentially ignited cotton waste placed on the unexposed surface, failing to meet the standard fire testing criterion (i) as mentioned above.

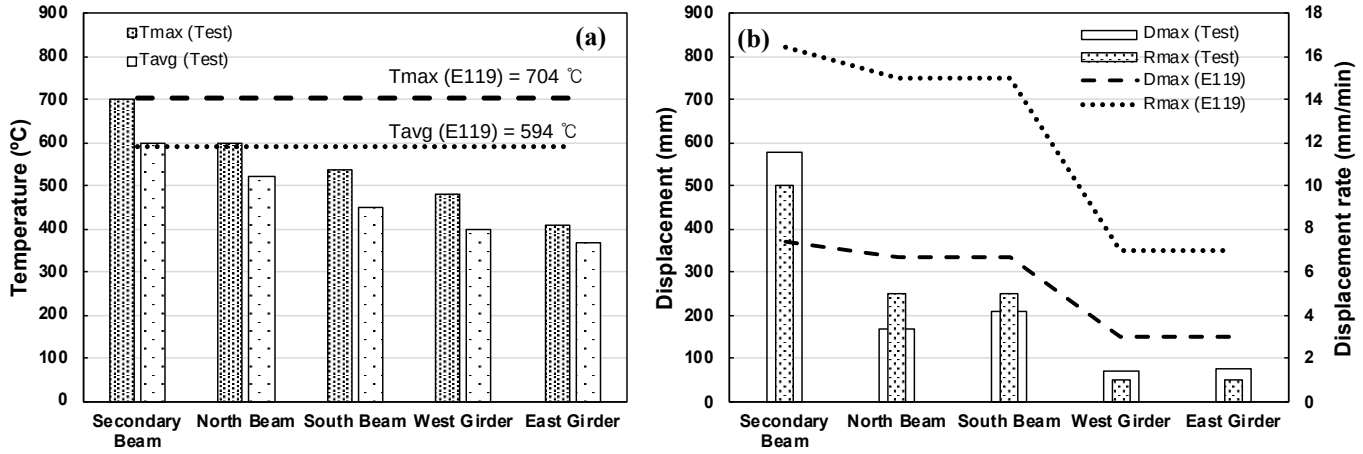

Figure 12. Comparisons of the test results with (a) limiting temperatures and (b) limiting displacements and displacement rates, where Dmax = maximum displacement and Rmax = maximum displacement rate.

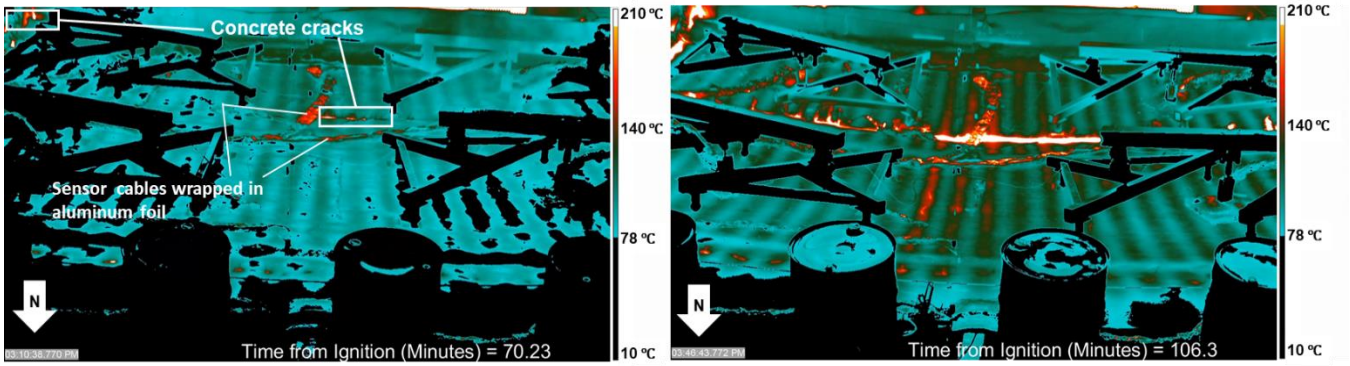

Figure 13. Thermal images of the top of the test floor slab at 70 min and 106 min after fire ignition.

5 SUMMARY & CONCLUSIONS

This paper presented the results of the first fire experiment on the 9.1 m by 6.1 m composite floor assembly situated on the first floor, south-edge bay of the two-story steel building designed and constructed following the current U.S. construction practice. The test floor assembly was subjected to a simulated compartment fire environment and mechanical loads conforming to the ASCE 7 load combination for extraordinary events (approximately 5 kPa including the assembly self-weight). The fire test conditions as well as thermal and structural responses of the test assembly to the combined effects of fire and mechanical loading are discussed and compared with the ASTM E119 acceptance criteria.

This test demonstrated that all fire-protected floor beams and girders met the ASTM E119 limiting temperatures. Also, these steel members never reached runaway at large vertical displacements (up to the ratio of L/16). The test floor assembly did not collapse after fire exposure, although some partial shear ruptures of connecting bolts were discovered after the test. However, the heated floor slab, during fire loading, exhibited a potential fire hazard before reaching a specified rating period, because of the use of the minimum code-compliant shrinkage reinforcement of 59 mm^2/m. The test floor slab began to crack along the interior edges (hogging moment regions) of the test column grid less than 30 min after ignition of the

fire. The centre cracks appeared around the midspan of the secondary beam at 70 min, which continued to propagate in the east-west direction. The glowing hot deck was exposed on the top of the slab through enlarged concrete cracks. This main breach was caused by ruptures of wire reinforcement in tension (due to catenary action) parallel with formed steel decking. Membrane action of the floor slab appeared not to be effective due to ruptures of the wire reinforcement across the east and west edges of the test-bay column grid and the subsequent loss of the east and west vertical supports of the concrete slab. This initial experiment suggests that the minimum required slab reinforcement currently allowed in the U.S. practice may not be sufficient to maintain the structural integrity of the composite floor assembly during structurally significant fire events.

Further study is recommended to evaluate the fire hazard of relatively 'thin' concrete slab details permitted in steel building constructions. As future work, the second test in this experimental program will study the influence of enhanced slab design (for both strength and ductility) on the fire performance of composite floor systems and the effectiveness of tensile membrane action, which is believed to significantly improve the fire safety of steel-framed buildings. The influence of slab reinforcement on the fire performance of composite floor systems is discussed in Choe et al. [16], which is the basis of the experimental design of the second test being planned in 2021.

ACKNOWLEDGMENT

This work was conducted as part of the project "Measurement of Structural Performance in Fire" under the NIST Engineering Laboratory's Fire Risk Reduction in Building Programs. The authors thank William Baker (Skidmore, Owings, and Merrill), Craig Beyler (Jensen Hughes), Luke Bisby (University of Edinburgh), Ian Burgess (University of Sheffield), Charles Carter (AISC), Charles Clifton (University of Auckland), Michael Engelhardt (University of Texas), Graeme Flint (Arup), Nestor Iwankiw (Jensen Hughes), Kevin LaMalva (Warringtonfire), Roberto Leon (Virginia Tech.), and Amit Varma (Purdue University) for their expert consultation. The authors also thank the NIST colleagues including Brian Story, Anthony Chakalis, Philip Deardorff, Laurean DeLauter, Marco Fernandez, Artur Chernovsky, Rodney Bryant, William Grosshandler, John Gross, Mina Seif, Ana Sauca, Fahim Sadek, Joseph Main, Chao Zhang, and Jonathan Weigand for their significant contributions to design, construction, and execution of this test program.

REFERENCES

1. Choe, L., Ramesh, S., Grosshandler, et al. Composite floor beams with simple shear connections subject to compartment fires: experimental evaluation, Journal of Structural Engineering, vol. 146, pp. 1-14, 2020. https://doi.org/10.1061/(ASCE)ST.1943-541X.0002627
2. Bundy M., Hamins, A., Gross, J., Grosshandler, W., Choe, L., Structural fire experimental capabilities at the NIST national fire research laboratory, Fire Technology, vol. 52 (4), pp. 959-966, 2016. https://doi.org/10.1007/s10694-015-0544-4
3. ASTM, Standard methods of fire test of building construction and materials, ASTM E119−19, ASTM International, West Conshohocken, PA, 2019.
4. Maluk, C., Bisby, L., Terrasi, G.P., Effects of polypropylene fibre type and dose on the propensity for heat-induced concrete spalling, Eng. Struct., vol. 141, pp. 584–595, 2017. https://doi.org/10.1016/j.engstruct.2017.03.058
5. Ramesh, S., Choe, L., Seif, M., et al. Compartment fire experiments on long-span composite beams with simple shear connections Part 1: experimental design and beam behavior at ambient temperature, Technical Note (NIST TN) - 2054, p141, 2019. https://dx.doi.org/10.6028/NIST.TN.2054
6. ASTM, Standard Test Method for Density, Absorption, and Voids in Hardened Concrete, ASTM C642 - 13, ASTM International, West Conshohocken, PA, 2013. https://doi.org/10.1520/C0642-13
7. SDI, C-2017 Standard for composite steel floor deck-slabs, Steel Deck Institute (SDI), 2017. http://www.sdi.org/wp-content/uploads/2017/02/ANSI-SDI-C-2017-Standard.pdf
8. ASCE, Minimum Design Loads and Associated Criteria for Buildings and Other Structures, ASCE/SEI 7-16, American Society of Civil Engineers, Reston, VA, 2016.

9. Choe, L., Ramesh, S., Hoehler, M. National fire research laboratory commissioning project: testing steel beams under localized fire exposure, Technical Note (NIST TN) – 1983, p117, 2018. https://dx.doi.org/10.6028/NIST.TN.1983
10. Zhang, C., Grosshandler W., Sauca A., and Choe L. Design of an ASTM E119 fire environment in a large compartment, Fire Technology, pp. 1–23, 2019. https://doi.org/10.1007/s10694-019-00924-7
11. Taylor B. and Kuyatt, C. Guidelines for Evaluating and Expressing the Uncertainty of NIST Measurement Results, Technical Note (NIST TN) – 1297, p24, 1994. https://doi.org/10.6028/NIST.TN.1297
12. Bryant, R. and Bundy, M. The NIST 20 MW calorimetry measurement system for large-fire research, Technical Note (NIST TN) – 2077, p68, 2019. https://doi.org/10.6028/NIST.TN.2077
13. ISO, ISO 834-2:2019 Fire-Resistance Tests – Elements of Building Construction (ISO, Geneva), 2019. Available at https://www.iso.org/standard/75137.html
14. Dai, X., Choe, L., Fischer, E., Clifton, C. Thermal response and capacity of beam and shear connections during a large compartment fire experiment. Proceeding of the 11th International Conference on Structures in Fire (SiF' 20), November 30 – December 02, 2020, University of Queensland, Australia (accepted for publication)
15. LaMalva, K., Bisby, L., Gales, J. et al. Rectification of "restrained vs unrestrained". Fire and Materials, pp 1-11, 2020. https://doi.rog/10.1002/fam.2771
16. Choe, L., Ramesh, S., Zhang, C., Clifton, C. Behaviour of composite floor assemblies subject to fire: Influence of slab reinforcement. Proceeding of 2021 Eurosteel Conference, September 1-3, 2021, University of Sheffield, United Kingdom (in production)